

*Full Length Research Paper*

# Physicochemical, spectroscopic and tableting properties of microcrystalline cellulose obtained from the African breadfruit seed hulls

Nwajiobi C. C.\*, Otaigbe J. O. E. and Oriji O.

Department of Pure and Industrial Chemistry, University of Port Harcourt, Rivers State, Nigeria.

Received 5 March, 2019; Accepted 9 April, 2019

This study evaluates the physicochemical, tableting and spectroscopic properties of microcrystalline cellulose obtained from the African breadfruit seed hulls. The seed hulls were dried, pulverized, sieved and digested with 2% w/v aqueous sodium hydroxide solution. The resultant pulp was further treated with 17.5% w/v NaOH solution and 2.5N hydrochloric acid to produce  $\alpha$ -cellulose and microcrystalline cellulose (BH-MCC), respectively. The prepared BH-MCC was characterized by studying their functional groups (using FT-IR), thermal stability using (TGA) and crystallinity index using (XRD). The results showed the composition of cellulose, hemicelluloses and lignin contents of the seed hulls were 39, 38 and 17%, respectively. The percentage yields of the isolated  $\alpha$ -cellulose and BH-MCC were 15.5 and 86.8%, respectively. The bulk, tapped and true densities were 0.33, 0.50 and 1.57 g/ml, respectively. Moisture content, angle of repose and swelling index were 5.3%, 28° and 29%, respectively. Tablets were produced by direct compression using BH-MCC and their analyses showed that the weight uniformity, hardness test, friability and disintegration time values were 190.3±4.2%, 4.95±0.83 kg/cm<sup>2</sup>, 0.04% and 31 s, respectively. The BH-MCC's tablets showed good compliance with the British Pharmacopeia (BP) specification, and can thus be considered useful as a binder and disintegrant in drug formulation.

**Key words:** Microcrystalline cellulose, African breadfruit seed hull, physicochemical, tableting, composition.

## INTRODUCTION

Agricultural activities and agro-based processing industries generate enormous wastes which are composed of large amounts of cellulosic fiber. Such lignocellulosic materials include bran and rice husk, straw from cereal, groundnut husk, coconut husk, etc. These wastes could pose disposal problems if not appropriately handled with consequent effects on the environment and the harmonious relationship between the biotic and

abiotic components of the ecosystem. Disposal of these wastes could be accomplished by incineration or other costly break-down system, open dumping, landfills, etc., all to the detriment of the environment (Nwabueze and Otunwa, 2006; Atuanya et al., 2012). Increased research has been focused on means of exploiting these wastes through various recycling methods, such as, a source of raw materials for industrial use, source of energy and

\*Corresponding author. E-mail: Cnwajiobi@yahoo.com.

major compounds like cellulose, gums, polymers, etc., and also as a major source of livestock feeds (Vora and Shah, 2015; Bakre and Ajala, 2012). This idea is in line with the recent interest taking into cognizance the concept of waste minimization and waste to wealth.

African breadfruit (*Treculia africana* Decne) is a monoecious evergreen fruit, in the family of Moraceae and order Urticales. It is native to tropical countries such as the West Indies, Ghana, Sierra Leone, Jamaica and Nigeria (Ejiofor et al., 1988; Emenonye, 2016). African breadfruit is characterized by its spherical shape, brownish yellow and spongy in texture when ripe, up to 18 inches in diameter, containing about 900 seeds scattered between the spongy pulps. The edible seeds are widely consumed among the Igbos in particular (Okonkwo and Ubani, 2007).

Cellulose is a major constituent of plant cell wall that is widely distributed in plant foods (Azubuike and Okhamafe, 2012). It is a polydisperse polymer of high molecular weight with the general formula  $(C_6H_{10}O_5)_n$  and consisting of long chain D-glucose units joined together by  $\beta(1\rightarrow4)$  glycosidic bonds (Vora and Shah, 2015). In nature, cellulose molecular chains are biosynthesized and self-assembled into microfibrils, which are composed of alternate crystalline and non-crystalline regions (Fernandes et al., 2011). These aggregated cellulose molecules are stabilized laterally by hydrogen bonds between the hydroxyl groups and oxygen of adjacent molecules (Nishiyama, 2009). The semi-crystalline regions of native cellulose can be readily hydrolyzed with almost no weight loss when subjected to strong acid hydrolysis in the preparation of microcrystalline cellulose (MCC) (Haafiz et al., 2013).

MCC is a purified, partially depolymerized cellulose which is used as an inert ingredient in oral pharmaceutical, nutraceutical, food products, cosmetics, paint, composite, etc. MCC is widely used as a binder, filler, bulking agent, disintegrant, stabilizer, thickener, texturizer, emulsifier as well as fat substitute. Woody plants and cotton are the major industrial sources of MCC but cost has made it imperative that other materials be investigated. Recently, non-woody biomass such as soybean husk, oat and rice hulls as well as sugar beet pulp (Hanna et al., 2001), groundnut shell and rice husk (Okhamafe et al., 1991), orange mesocarp (Ejikeme, 2008), mango kernel (Nwadiogbu et al., 2015), bagasse and maize cob (Okhamafe et al., 1995), water gourd (Achor et al., 2014), *Pennisetum purpureum* (Ogbonna et al., 2016), coffee husk (Collazo-Bigliardi et al., 2018), roselle fibers (Lau et al., 2017), and *Dendrocalamus asper* (Yusrina et al., 2018) have been used as precursors for the preparation of the MCC. According to the study by Khali et al. (2018), the MCC obtained from sacred Bali bamboo was considered to be useful as a reinforcing filler in seaweed-based composite film (Abdul Khali et al., 2018). Liu et al., (2018) employed alkaline hydrogen peroxide liquor and acid hydrolysis in the

isolation of MCC from pomelo peel. Results showed that the MCC was found to be suitable for use as food stabilizing and pharmaceutical additives.

There is a dearth of information in the literature on the production of cellulose and microcrystalline cellulose using the seed hull of African breadfruit. Accordingly, this was performed to synthesize microcrystalline cellulose from the seed hulls of African breadfruit and evaluate its physicochemical and tableting properties.

## MATERIALS AND METHODS

### Raw materials

#### Cellulosic precursor

African breadfruit (*T. africana* Decne.) was selected as a precursor for its seed hulls. The breadfruit seed hulls (BSH) were obtained from Nkwo market in Igboukwu town, Anambra State, Nigeria. The seed hulls were dried, screened and milled using an electric grinder then allowed to cool to room temperature. The seed-hull powder was sieved using 2.0 mm laboratory test sieve (Endecotts Ltd., London, England).

#### Compositional analysis

The procedural technique reported by Nwajiobi et al. (2018) was adopted in the lignin, cellulose and hemicellulose content determination of the substrate.

#### Isolation of alpha cellulose

A slight modification of the method by Ohwoavworhwa et al. (2005) was adopted. 1000 g of the sieved fraction of the seed-hull was delignified using 5.550 L of 2% w/v aqueous NaOH solution in a stainless steel container immersed in a water bath [Precisidig (6001197) JP Selecta water bath] which was maintained at 80°C for 3 h. After thorough washing and filtration, the wet mass of the delignified seed-hull was treated with 2 L of 3.5% w/v aqueous NaOCl solution for 30 min at 80°C. The resulting bleached seed hull was further digested with 1.8 L of 17.5% w/v NaOH solution at 80°C for 1 h. The bleaching process was then completed by subjecting the alpha cellulose in its crude form by treating with 1 L of 1:1 dilution of 3.5% w/v NaOCl solution repeatedly at 80°C for 1 h. This was followed by washing with water until the washings were neutral to litmus paper. The product was manually squeezed through a muslin cloth to obtain a small mass which was oven-dried using JP Selecta Digiheat Oven at 65±1.5°C for 12 h. The preparation method as reported by Nwajiobi et al. (2018) was adopted in the production of microcrystalline cellulose (BH-MCC).

#### Physicochemical analysis

##### Characterization of MCC

Identification, organoleptic properties, starch, dextrin and solubility tests were carried out according to BP specifications (Annon, 2009).

##### pH

This was determined using pH meter (pHep® pocket-sized pH

meter) by shaking 1 g of MCC with 50 ml of distilled water for 5 min and taking the pH of the supernatant liquid.

#### **Moisture content**

Two grams of the powdered sample was weighed, transferred into a petri dish and then oven-dried for 3 h at 105°C to a constant weight. The moisture content (%) was then computed based on the initial air-dried weight.

#### **Bulk density ( $D_B$ )**

Five grams of MCC sample was weighed and transferred into a 50 ml dry measuring cylinder. The volume occupied by the sample was noted as the bulk volume and the bulk density was determined by dividing the mass of the material by the bulk volume as expressed (Umeh et al., 2014):

$$\text{Bulk density} = [M / V_B]$$

where M is the mass of the sample and  $V_B$  is the bulk volume of sample

#### **Tapped density ( $D_{Ta}$ )**

The measuring cylinder containing 5 g of MCC was then tapped on a wooden platform by dropping the cylinder from a height of 1 inch at 2 s intervals until there was no observable change in volume. The volume occupied by the material was recorded as the tapped volume. The tapped density was determined using the expression:

$$\text{Tapped density } (D_{Ta}) = [M / V_T]$$

where M is the mass of the sample and  $V_T$  is the tapped volume of sample.

#### **True density ( $D_{Tr}$ )**

The true density was determined by the liquid displacement method by completely immersing the sample in a pycnometer bottle (26 ml) capacity using xylene as the immersion fluid. The volume of the liquid that was displaced was measured and the density was computed according to the following equation:

$$D_{Tr} = [w / \{(a + w) - b\} \times SG]$$

where w is the weight of powder, SG is specific gravity of xylene, a represents sum of weights of the bottle and solvent and b represents the sum of weights of bottle, solvent and the MCC powder.

#### **Hausner's ratio ( $H_r$ )**

This is calculated as the ratio of tapped density to bulk density of the sample (Ohwoavworhwa et al., 2004) as follows:

$$H_r = D_{Ta} / D_B$$

#### **Powder porosity ( $P_p$ )**

This was determined from the values of true and bulk densities when fitted into the equation:

$$e = 1 - D_B / D_{Tr} \times 100$$

where  $D_B$  is the bulk density,  $D_{Tr}$  is the true density and e is the porosity (Achor et al., 2014).

#### **Compressibility index ( $I_c$ )**

This was calculated by fitting bulk and tapped densities data into the equation as expressed by (Ohwoavworhwa et al., 2004) as follows:

$$\text{Compressibility index } (C\%) = [(D_{Ta} - D_B) / D_{Ta}] \times 100$$

#### **Hydration capacity ( $H_c$ )**

The method of Kornblum and Stoopak (1973) was used to determine the  $H_c$  of MCC. The hydration capacity was determined as the ratio of the weight of the sediment to the oven-dried weight.

$$HC = [(\text{weight of sediment} - \text{weight of tube}) / \text{oven-dried}]$$

#### **Swelling capacity (Swellability)**

This was determined at the same time as the hydration capacity determination using the method reported by Ohwoavworhwa and Adelakun (2010) and was calculated as follows:

$$\text{Swelling capacity} = [(V_2 - V_1) / V_1]$$

where  $V_1$  = tapped volume occupied by the sample prior to hydration and  $V_2$  = volume occupied by sample after hydration.

#### **Angle of repose ( $a$ )**

The procedure as reported by Achor et al., (2014) was used to determine the angle of repose. The mean diameters of the base of the powder cones were determined and the tangent of the angle of repose was calculated using the equation:

$$\tan a = 2h/D$$

where h is the height of the heap of powder and D is the diameter of the base of the heap of powder.

#### **Moisture sorption capacity**

One gram of the sample was weighed and evenly distributed over the surface of a 10 cm Petri dish. The sample was placed in a large desiccator containing distilled water in its reservoir and the weight gained by the exposed sample at 24-h interval was recorded. The amount of water sorbed was calculated from the weight difference:

$$[(W_2 - W_1) / W_1] \times 100$$

where  $W_1$  is the weight of the samples before exposure and  $W_2$  is the weight of the sample after exposure.

#### **Particle size analysis**

This was determined using a trinocular microscope (SXY-m50) and an s-viewer application for the sample size of 100 particles.

**Scanning electron microscopy (SEM)**

The SEM was carried out using SEM, JSM 5400 (JEOL Ltd., Japan) at an accelerated voltage of 10 kV.

**Fourier transform (FTIR) spectroscopy**

The FTIR spectroscopy of the sample was characterized using {model: Shimadzu FTIR-8400S (650-4000  $\text{cm}^{-1}$ )}.

**Thermogravimetric analysis (TGA)**

The TGA analysis was carried out to determine thermal stability or behaviour of the sample using Perkin-Elmer Thermal Analysis controller at a heating rate of 10°C/min in nitrogen atmosphere.

**X-ray diffraction (XRD)**

This was carried out using a Phillips X-ray diffractometer. The scanning region of the diffraction angle  $2\theta$  was from 5 to 65° and the crystallinity was calculated as follows (Qian et al., 2012):

$$\text{Relative crystallinity} = (I_{\text{crystalline}} - I_{\text{amorphous}}) / I_{\text{crystalline}} \times 100\%$$

where  $I_{\text{crystallinity}}$  is identified with the intensity at 22.5° and  $I_{\text{amorphous}}$  is the intensity at 18.3°.

**Preparation of tablets**

Tablets were prepared by manually feeding the MCC powders to the tablet press through the hopper and then compressed at the pressure of 5.5 MPa using a flat faced punch fitted to a single punch tableting machine (Model C, Carver Inc., Wisconsin, U.S.A) and the target tablet was 200 mg.

**Evaluation of tablet properties**

The properties of the tablets were determined to ensure compliance with Pharmacopoeia standard. The underlisted tests were performed.

**Weight uniformity**

Twenty tablets from each batch were randomly selected and individually weighed, the average weight was then determined. The percentage deviation of each tablet weight from the mean weight was determined and the conformity or non-conformity of the tablet batch to official weight uniformity standards were also determined (Ogbonna et al., 2016).

**Hardness test**

Ten tablets from each batch were used for the hardness test. Each of the tablets to be tested was placed between the spindle and the anvil (Monsato tester) and then pressure was applied by turning the knob just sufficient to hold the tablet in position. The reading on the pointer on the scale was adjusted to zero and pressure was then increased as uniformly as possible until the tablets cracked and the pointer value was read, which indicated the pressure required by the tablets to break. The mean and standard deviations of the values obtained were determined.

**Friability test**

Ten tablets were selected randomly from each batch and collectively weighed. The weighed tablets were subjected to abrasive shock at 25 rpm for 4 min using a twin drum electronic friabilator (Erweka, Germany). At the end, the tablets were de-dusted and re-weighed and the percentage weight loss was calculated (Ofoefule, 2006).

$$\% \text{ Friability} = 100 (1 - W / W_0)$$

where  $W_0$  is the initial weight and  $W$  is the final weight of the tablets.

**Disintegration time test**

The disintegration time was determined by placing six tablets obtained from each batch in the six Perspex tubes in the basket assembled and held with a glass immersed in a freshly prepared 500 mL volume of 0.1N HCl solution which was heated and maintained at 37±1°C (Erweka ZT-300, Germany). The time taken for the tablet to break up into small aggregates was recorded as the disintegration time (Anonymous, 2009).

**RESULTS AND DISCUSSION**

The composition of lignocellulosic biomass has tremendous effect on the efficiency of cellulose hydrolysis and bioconversion. This explains why knowledge of biomass composition as well as selection of biomass treatment is very important (Mood et al., 2013). Other major factors limiting biomass conversion is the degree of crystallinity of cellulose, cellulose covered by hemicellulose and lignin content. The compositional analyses indicate that the cellulose, hemicellulose and lignin content of Breadfruit seed hull are 39, 38, and 17%, respectively (Table 1). The 15.5% w/w yield of the  $\alpha$ -cellulose isolated from the breadfruit seed hull differed from the 6% w/w reported for Pennisetum purpurea (Ogbonna et al., 2016), 10.5% w/w reported for maize husk (Bakre and Ajala, 2012) as well as that reported for sugarcane scrappings (Gbenga and Fatimah, 2014). The BH-MCC yield obtained from the  $\alpha$ -cellulose was 86.80% w/w. Thus, BH-MCC yield from the starting material was approximately 14% w/w, a reduction in value which was expected. This is because a good amount of non-crystalline regions are solubilized and eliminated during acid hydrolysis and washing steps.

The organoleptic characteristics of the prepared BH-MCC (Table 2) were found to be satisfactory as the product was odourless, tasteless, off-white granular powder. The identification test gave a violet-blue colour while the starch and dextrin test did not indicate any change in colour. Thus, the prepared MCC met the specifications as established by the BP (Annon, 2009). The result from the solubility test showed that BH-MCC was insoluble in the specified solvents.

The value of the water soluble substances ( $\leq 0.44\%$ ) was not in conformity with the standard ( $\leq 0.25\%$  or  $\leq 12.5$

**Table 1.** Compositional analyses.

Component	Percentage
Cellulose	39
Hemicellulose	38
Lignin	17

**Table 2.** Identification and organoleptic test.

Test	BH-MCC
Organoleptic properties	Off-white, Odorless, tasteless granular powder
Identification	Turns violet blue with iodinated Zinc chloride
Starch and Dextrin	Negative
pH	5.5 (0.06)
Water soluble substance	≤ 0.44%
Solubility (n-hexane, water, acetone, ethanol)	Insoluble
Microscopy	Irregularly spherical shaped fibrous structure

mg) as specified by the BP. The high value obtained may be due to lower crystal phase appearance of the MCC barring the impurities caused by the preparation procedure, some sugar components of hemicellulose such as xylose (predominant in hardwoods) and mannose (Predominant in softwoods) are possible water soluble substances (Baehr et al., 1991; Lanz, 2006). Consequently, there could be traces of sugar components of hemicellulose which may also be present in non-woody materials. The pH value (5.5) can be enhanced towards neutralization by excess of washing with distilled water. However, the obtained value is in accordance with the specification (5-7.5) of the BP (Anonymous, 2009).

The value of moisture content obtained was lower than the maximum allowable limit of 8% (Anonymous, 1993), 7% (Anonymous, 2009) and was by far greater than 1.5% reported for Avicel PH-112 and 113 (Hanna et al., 2001), 4.3 and 4.9% for luffa cylindrical (Ohwoavworhua et al., 2004) and orange mesocarp (Ejikeme, 2008), respectively but less than 5.7, 9 and 7.6% reported for corn cobs (Azubuike and Okhamafe, 2012), water gourd (Achor et al., 2014) and Avicel PH 101 (Achor et al., 2014), respectively. Bhimte and Tayada (2007) reported values ranging from 3.96 to 5.06% after heating for 8 h at 105°C. The presence of substantial amount of water encourages microbial growth and deterioration by hydrolysis. Thus when the moisture of MCC exceeds 5%, water molecules function as plasticizer thereby affecting the mechanical properties of MCC which leads to lower tensile strength of MCC tablets (Wu et al., 2011; Pachau et al., 2014). However, the moisture content values can be easily reduced by drying for longer periods or at higher temperatures as well as by using additional assisting aids, such as, air forced circulation.

Bulk density depends on the particles packing behavior which changes as the powder consolidates (Musiliu et al., 2014). Higher bulk density implies the need for larger amount for compressing tablet which is favourable in tableting due to reduction in the fill volume or so-called lower loading volume (Pachau et al., 2014). Tapped density also measures how well a powder can be packed into a confined space on repeated tapping. The BH-MCC values for the bulk and tapped densities shown in Table 3 indicate that it has high bulk and tapped densities. Small particle size and low moisture content have been suggested to lead to high bulk density (Ejikeme, 2008). The bulk density of BH-MCC was greater than that reported for orange mesocarp (0.42 g/ml) (Ejikeme, 2008), *P. purpureum* (0.40 g/ml) (Ogbonna et al., 2016), Muli bamboo (0.35 g/ml) (Pachau et al., 2014) and *Sorghum caudatum* (0.27 g/ml) (Ohwoavvorhua and Adelakun, 2010). Thus, BH-MCC may have better flow property, although it would require the need for larger amount for compression in tablet manufacturing.

True density measures the density of a solid material with the exclusion of any open and closed pores. This can be indicative of the closeness of the material to the crystalline state or the proportions of a binary mixture (Achor et al., 2014). High true density indicates high crystallinity which is in accordance with report by Stamm (1964), which states that the degree of crystallinity of cellulose increases directly with true density when determined in a non-polar solvent (Stamm, 1964). The true density value of BH-MCC (1.57 g/ml) was greater than that reported for Mango kernel (1.36 g/ml) (Nwadiogbu et al., 2015), sugar palm bunches (1.47 g/ml) by Musiliu et al. (2014) and slightly above that reported for Avicel PH 101 (1.50 g/ml) (Achor et al., 2014). Thus, it might exhibit better compressibility and possess higher

**Table 3.** Powder properties of microcrystalline cellulose (BH-MCC).

Parameter	BH-MCC
Moisture content (%)	5.3 (0.34)
Bulk density (g/ml)	0.33 (0.006)
Tapped density (g/ml)	0.50 (0)
True density (g/ml)	1.57 (0.01)
Angle of repose ( $\Phi^0$ )	28 (0.80)
Compressibility index (%)	34
Hausner's ratio	1.52
Porosity (%)	78.65 (0.26)
Swelling capacity (%)	28.99 (1.78)
Moisture sorption capacity (%)	45
Hydration capacity	2.33 (0.12)
Average particle size ( $\mu\text{m}$ )	8.213 (2.83)

\*Value is mean and standard deviation is in parenthesis, number of replicate=3.

crystallinity.

Angle of repose is referred to the maximum angle between pile of powder and the horizontal plane and its measure gives qualitative assessment of frictional forces in powders. Angles of up to  $40^\circ$  indicate reasonable flow potential of solid powders where  $30$  to  $40^\circ$  is passable,  $25$  to  $30^\circ$  is good and less than  $25^\circ$  is excellent, whereas angles greater than  $50^\circ$  show poor or absence of flow (Fowler, 2000; Azubuike and Okhamafe, 2012). The angle of repose value reported for *Saccharum officinarum* ( $25.50^\circ$ ) (Musiliu et al., 2014) shows moderate flow potential (that is, lie around the threshold of reasonable flow potential) than that reported for BH-MCC, whereas the lower angle of repose value ( $20.47^\circ$ ) for sugar palm bunches (Sumaiyah et al., 2016) suggests superior flow properties.

Compressibility or Carr's index, Hausner ratio and angle of repose are indirect measurements for powder flowability for which small value indicates better flowability (Wu et al., 2011). The Hausner's index is indicative of interparticulate friction between particles while the Carr's index indicates the tendency or aptitude of a material to diminish in volume (Rubinstein, 1996; Achor et al., 2014). Values of the Carr's index ranging from 5-15, 12-16, 18-21, 23-25 and 33-38 indicate excellent, good, fair, poor and very poor flow properties of the material, respectively. The Carr's index of BH-MCC (34%) is greater than those reported for water gourd (23.5, 11.38, 28.86, 19.1 and 27.33%) by Achor et al. (2014), sugar palm bunches (Musiliu et al., 2014), corn cob (Azubuike and Okhamafe, 2012), orange mesocarp (Ejikeme, 2008), mango kernel (Nwadiogbu et al., 2015) and *P. purpureum* (Ogbonna et al., 2016), respectively. Based on the Carr's index results, the BH-MCC has poor flow properties.

On the other hand, Hausner's ratio value of less than 1.20 indicates good flowability whereas a value of 1.50 or

higher suggests that the material will have poor flow properties. The value obtained for the Hausner's ratio of BH-MCC (1.52) showed that it has poor flow properties. Accordingly, the poor flowability behaviors are obvious from the Hausner's ratio and Carr's index results. The flowability results obtained for BH-MCC were not unusual, as other authors had reported similar values for different MCC (Ejikeme, 2008; Bhimte and Tayade, 2007; Ohwoavworhwa and Adelokun, 2005; Oluwasina et al., 2014).

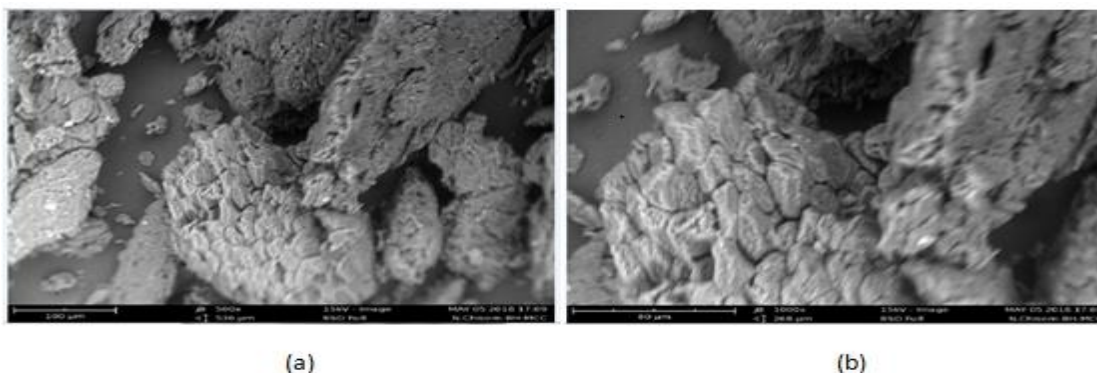
Porosity is the voids between and within particles. The space between particles is known as void and the volume occupied by this void is called void volume. The high value of total porosity of BH-MCC (78.65%) corresponds with the high tapped density. Degree of material densification correlates to its porosity which is a function of the void volume (Mohammed et al., 2009; Olorunsola et al., 2016). Swelling index property is essential specifically for MCC as its disintegration property is mainly attributed to the swelling of MCC particles and the decrease of bonding forces holding them together. The swellability value of BH-MCC showed that there was increase in volume after water absorption. It is probably that only a small portion of absorbed water actually penetrated the individual cellulose particles forcing them to swell and the remaining bulk would exist in free-state between the particles.

Moisture sorption capacity assesses the materials sensitivity toward moisture. It was reported that the crystallite portion of cellulose does not adsorb water and that the magnitude of water adsorption by cellulose is proportional to the amount of amorphous cellulose present (Stamm, 1964). As a result of the nature of MCC being sensitive to the atmospheric humidity, its storage should be done in a tightly sealed container.

Hydration capacity is the ability of materials to absorb water and hold it even after treatment with external forces

**Table 4.** Tableting properties of BH-MCC.

Parameter	BH-MCC	BP standard
Weight uniformity	$\pm 4.19\%$	$\pm 7.5\%$
Hardness ( $\text{kg}/\text{cm}^2$ )	$4.95 \pm 0.83$	3-8
Friability (%)	0.04	$\leq 1$
Disintegration (min)	31 s	$\leq 15$

**Figure 1.** Scanning electron micrograph of BH-MCC (a) 500x and (b) 1000x.

such as pressing, centrifugation or heating. The level and extent of hydration capacity of polymers is directly related to its porosity. The hydration capacity of a material is a measure of the amount of water that can be taken-up by the material (Isah et al., 2012; Olorunsola et al., 2016). The hydration capacity values of 6.55 and 5.96 reported for water gourd and Avicel PH 101 (Achor et al., 2014) were greater than that of BH-MCC (2.33).

The result of weight uniformity or variation test of BH-MCC's tablet conformed to the specifications of British Pharmacopoeia for uncoated tablets. This states that tablets with average weight of more than 80 mg or less than 250 mg will have average weight deviation of ( $\pm 7.5\%$ ) and not more than two of the tablets differed from the average weight by more than the percentage error listed in Table 4, just as no tablet differed by more than double of that percentage error (Anonymous, 2009). Thus, the maximum average weight variation obtained was  $\pm 4.2\%$  which is within the acceptable weight variation of  $\pm 7.5\%$ . Thus, all the tablets passed the weight variation test. The hardness values of the tablets were in the range of 4.1 to  $5.8 \text{ kg}/\text{cm}^2$ , which is above the limit of not less than  $3.0 \text{ kg}/\text{cm}^2$ . Friability describes the effect of physical impact on the tablet during handling, packaging and transportation. None of the tablets showed friability value of more than 0.04%, which is less than the ideal limit 1%. Thus, the integrity of the tablets is assured. The disintegration test of BH-MCC's tablet was 31 s which is less than the ideal limit of 15 min.

Figure 1a and b shows the scanning electron

micrograph images of the BH-MCC at different magnifications. It was observed that the BH-MCC showed irregular spherical shaped fibre structures which existed in large aggregated crystal packed form and with a rough surface morphology. Surface cracks which resulted to the roughness of the MCC were also observed. This may be due to the removal of amorphous hemicellulose and lignin within the microfibrils (Johar et al., 2012). The roughness of MCC supports the production of nanocrystals through hydrolysis (Mathew et al., 2006). This observation is not in agreement with the shape and surface characteristics of the commercially available MCC previously reported by Ohwoavworhwa et al., (2004), Haafiz et al., (2013) and Avicel PH 101 by Pachuau et al. (2013) which existed as non-aggregated, individual fibres, but it is in conformity with the findings of Nwadiogbu et al. (2015), Rosnah et al., (2009), etc. The difference in the particle shape may be due to the different cellulose source as well as the hydrolysis and processing conditions (Lee et al., 2009; Haafiz et al., 2013).

#### Fourier-transform infrared spectroscopy (FTIR)

From Figure 2, two major absorbance regions were found at high wavenumbers ( $2900\text{-}3600 \text{ cm}^{-1}$ ) and low wavenumbers ( $600\text{-}1700 \text{ cm}^{-1}$ ) as displayed by the MCC sample reported by Rosa et al. (2012). Distinct absorption bands located at  $2916$  and  $1427 \text{ cm}^{-1}$  regions

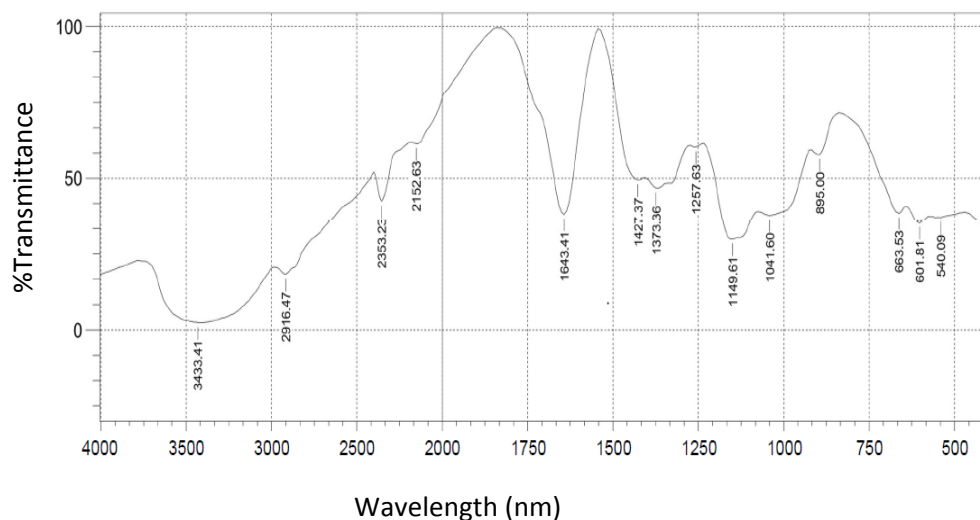


Figure 2. FT-IR Spectra obtained of BH-MCC.

indicate that the sample is characterized by high level of orderliness of macromolecules (Zhbakov, 1962). The broad absorption band at  $3433\text{ cm}^{-1}$  is due to the intermolecular and intramolecular hydrogen bonded O–H stretching vibration and the band at  $2917\text{ cm}^{-1}$  is due to the presence of  $-\text{CH}_2$  groups present in the MCC samples (Haafiz et al., 2013; Adel et al., 2011). The absorption band located at  $1643\text{ cm}^{-1}$  is indicative of vibration of absorbed water molecules which is due to the strong cellulose-water interaction as well as the presence of small amounts of hemicellulose (Adel et al., 2011). Rosa et al. (2012) related this band to the bending modes of water molecules. The absence of peaks located in the range of  $1509$  to  $1609\text{ cm}^{-1}$  is indicative of complete removal of lignin (Rosa et al., 2012). The band at  $1700$  to  $1740\text{ cm}^{-1}$  which corresponds to either the acetyl or uronic ester groups of hemicellulose or the ester linkage of the carboxylic group of ferulic and p-coumaric acids of lignin and/or hemicelluloses (Nuruddin et al., 2011; Haafiz et al., 2013) is absent in BH-MCC sample. The peak at  $1427\text{ cm}^{-1}$  is due to the  $-\text{CH}_2-$  bending. According to Kalita et al., (2013), the absorption band is also associated with intermolecular hydrogen bonds at C-6 also known as the crystallinity band, the increase in their intensity shows a higher degree of crystallinity. The peak associated with the C-O-C stretching at the  $\beta$  (1 $\rightarrow$ 4) glycosidic linkages was located at  $1149\text{ cm}^{-1}$ . The band at  $1041\text{ cm}^{-1}$  shows C-O stretching vibration at C-3, C-C stretching and C-O stretching at C-6 while the absorption spectra  $895\text{ cm}^{-1}$  is attributed to the asymmetric out of plane ring stretching C-H vibration of cellulose which corresponds to the  $\beta$ -glycosidic linkage. Accordingly, it can be confirmed that the BH-MCC are composed mainly of crystalline cellulose I while content of amorphous cellulose is eliminated upon the hydrolysis process applied.

### X-ray diffraction (XRD)

Figure 3 was carried out to determine the crystallinity index. It is widely recognized that fibrous cellulose consist of both ordered and less ordered region (Klemm et al., 2005). The X-ray diffractogram of crystalline polymers produce peaks, while the amorphous polymers tend to produce a widened or blunt base. The X-ray diffraction pattern of BH-MCC sample (Figure 3) showed strong peaks at  $2\theta = 16, 22.5$  and  $34.5^\circ$ , respectively with the sharper diffraction peak at  $22.5^\circ$  indicating an increase in crystallinity. The sample has similar diffraction pattern typical of native cellulose I which is indicated by the non-existence of doublet in the intensity of the main peak located at  $22.5^\circ$  (Rosa et al., 2012; Haafiz et al., 2013). The BH-MCC has 76% crystallinity index which is as a result of both the alkaline treatment and, in particular the acid hydrolysis. This caused significant increase in the cellulose fraction value by prompting hydrolytic cleavage of glycosidic bonds which then leads to rearrangement of cellulose molecules (Haafiz et al., 2013). High crystallinity indicates an ordered, compact molecular structure which translates to dense particles, whereas, lower crystallinity implies a more disordered structure, resulting in more amorphous powder (Shanmugam et al., 2014). Higher crystallinity also improves the tensile strength towards fibre formation which ultimately enhances the mechanical properties of composite materials due to the increase in the rigidity of the cellulose structure (Beg et al., 2015; Rosa et al., 2012).

### Thermal analysis of the BH-MCC

Figure 4 shows thermogravimetric analysis (TGA) and the derivative thermogram curve (DTG). The investigation

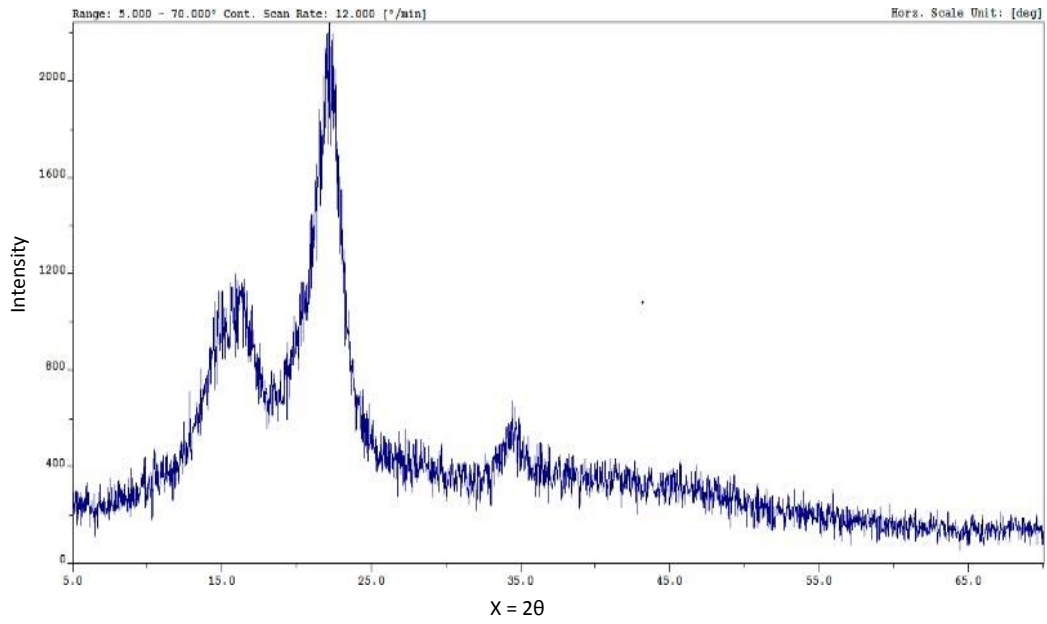


Figure 3. X-ray diffractogram of BH-MCC.

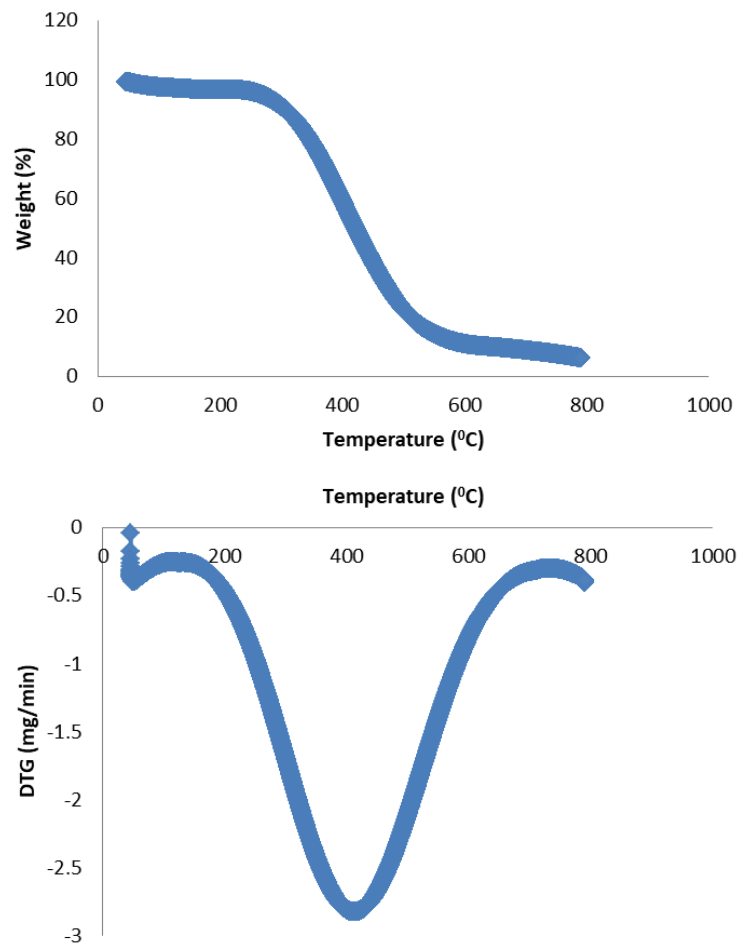


Figure 4. TGA/DTG curve of BH-MCC.

of the thermal stability is vital in determining the application of polymers in the production of biocomposite which operates at a very high temperature (Haafiz et al., 2013). The TGA curve indicates a two-phase degradation with an initial weight loss below 150°C which is attributed to evaporation of both absorbed and external water bonded by surface tension (Adel et al., 2011). The presence of this endotherm on thermograms of cellulosic materials is as a result of cellulose-water interactions due to the hydroxyl groups. The major decomposition peak of the sample which is labeled ( $T_{max}$ ) can be seen in the derivative weight loss curve. The decomposition peak temperature 391°C shows the point of cellulose degradation. The high degradation temperature may be attributed to the surface morphology which is in aggregated crystal packed form as shown in Figure 1. Raveendran et al. (1995) reported the prominent stages that can be observed in DTG, such as, evaporation of moisture below 100°C, decomposition of hemicellulose between 250 and 350°C, decomposition of cellulose between 350 and 500°C and lignin decomposition beyond 500°C. Cellulose degradation involves the decomposition of the glycosyl units which results to the evolution of gases. The thermo-gravimetric curves (TGA) of the prepared MCC is very similar to that of MCC prepared from bamboo and oil palm biomass residue as reported by Pachau et al. (2014) and Haafiz et al., (2013), respectively. The residue obtained for the sample at 800°C is 5.79%. This high char residue of the sample may be attributed to the decrease of disordered regions and increase of the hydrogen bonds in the ordered region as a result of the acid hydrolysis carried out to obtain the MCC. According to Mandal and Chakrabarty (2011), the high amount of crystallinity of cellulose I is intrinsically flame retardant and the sample can be said to have good thermal resistance which may be useful as reinforcing filler for making composites.

## Conclusion

The overall analysis of microcrystalline cellulose obtained from the seed hull of African breadfruit indicates that it is reliable and has some satisfactory physicochemical and tableting properties. Therefore, it can be recommended for use as an alternative source of producing microcrystalline cellulose where it can be applied as a disintegrant and binder in producing tablets by direct compression. The thermal properties showed that it has good thermal stability and can be incorporated in making composites.

## CONFLICT OF INTERESTS

The authors have not declared any conflict of interests.

## REFERENCES

Abdul Khali HPS, Lai TK, Tye YY, Paridah MT, Fazita NMR, Azniwati

- AA, Dungani R, Rizal S (2018). Preparation and characterization of microcrystalline cellulose from sacred bali-bamboo as reinforcing filler in seaweed-based composite film. *Fiber and Polymers* 19(2):423-434.
- Achor M, Oyeniyi YJ, Yahaya A (2014). Extraction and characterization of microcrystalline cellulose obtained from the back of the fruit of *Lageriana siceraria* (water gourd). *Journal of Applied Pharmaceutical Science* 4(1):57-60.
- Adel AM, El-Wahab ZHA, Ibrahim AA, Al-Shemy MT (2011). Characterization of microcrystalline cellulose prepared from lignocellulosic materials. Part II: physicochemical properties. *Carbohydrate Polymers* 83(2):676-687.
- Anonymous (1993). *British Pharmacopoeia*. HMSO Press, London, vol 1, p 53
- Anonymous (2009). *British Pharmacopoeia*. Volume 11. Her Majesty Stationery Office, University Press Cambridge. pp A366-A327.
- Atuanya CU, Aigbodion VS, Nwigbo U (2012). Characterization of breadfruit seed hull ash for potential utilization in metal matrix composites for automotive application. *Peoples Journal of Science and Technology* 2(1):2249-5847.
- Azubuike CP, Okhamafe OA (2012). Physicochemical, spectroscopic and thermal properties of microcrystalline cellulose derived from corn cobs. *International Journal of Recycling of organic waste in Agriculture* 1:9.
- Baehr M, Fuhrer C, Puls P (1991). Molecular weight distribution, hemicellulose content and batch conformity of pharmaceutical cellulose powders. *European Journal of Pharmaceutics and Biopharmaceutics* 37(3):136-141.
- Bakre LG, Ajala OJ (2012). Preliminary physicochemical characterisation of powdered *Zea Mays*' husk, silk and cellulose derived from *Zea mays* husk. *Nigerian Journal of Pharmaceutical Science* 11(2):21-30.
- Beg M, Rosli M, Ramli R, Junadi N (2015). Microcrystalline cellulose (MCC) from oil palm empty fruit bunch (EFB) fiber via simultaneous ultrasonic and alkali treatment. *International Journal of Chemical, Molecular, Nuclear, Materials and Metallurgical Engineering* 9(1):8-11.
- Bhimte NA, Tayade PT (2007). Evaluation of microcrystalline cellulose prepared from sisal fibers as tablet excipient: A technical note. *Journal of the American Association of Pharmaceutical Scientists* 8(1):E1-E7.
- Collazo-Bigliardi S, Otega-Toro R, Chiralt BA (2018). Isolation and characterization of microcrystalline and cellulose nanocrystals from coffee husk and comparative study with rice husk. *Carbohydrate Polymers* 191:205-215.
- Ejikeme PM (2008). Investigation of the physicochemical properties of microcrystalline cellulose from agricultural wastes orange mesocarp. *Cellulose* 15(1):141-147.
- Ejiofor MAN, Obianuju OR, Okafor JC (1988). Diversifying of African breadfruit as food and feeding stuff. *International Tree Crops Journal* 5(3):125-134.
- Emenonye AG (2016): Extent of processing effect on the proximate and mineral composition of African Breadfruit (*Treculiaafricana*) seed. *International Journal of Science and Technology* 4(4):6-10.
- Fernandes AN, Thomas LH, Altaner CM, Callow P, Forsyth VT, Apperley DC, Kennedy CJ, Jarvis MC (2011). Nanostructure of cellulose microfibrils in spruce wood. *Proceedings of the National Academy of Sciences of the United States of America* 108(470):195-1203.
- Fowler HW (2000). Powder flow and compaction. In: Carter S. J (ed) Cooper and Gunn's tutorial pharmacy, 6th ed. CBS Publishers, Delhi.
- Gbenga BL, Fatimah OK (2014). Investigation of  $\alpha$ -cellulose content of sugarcane scrappings and Bagasse as tablet disintegrant. *Journal of Basic and Applied Science* 10:142-148.
- Haafiz MK, Eichhorn SJ, Hassan AM, Jawaid M (2013). Isolation and characterisation of microcrystalline from oil palm biomass residue. *Carbohydrate Polymers* 93(2):628-634.
- Hanna M, Blby G, Miladinove V (2001). Production of microcrystalline cellulose by reactive extrusion, US Patent 6, 228 ,213. <https://patents.justia.com/patent/6228213>
- Isah AB, Olorunsola EO, Zaman YE (2012). Physicochemical properties of *Borassumachthiopum* starch. *Asian Journal Pharmaceutical and*

- Clinical Research 5(3):132-134.
- Johar N, Ahmad I, Dufresne A (2012). Extraction, preparation and characterization of cellulose fibres and nanocrystals from rice husk. *Industrial Crops and Products* 37(1):93-99.
- Kalita RD, Nath Y, Ochubiojo ME, Buragohain AK (2013). Extraction and characterization of microcrystalline cellulose from fodder grass; *Setaria glauca* (L) P. Beauv, and its potential as a drug delivery vehicle for isoniazid, a first line antituberculosis drug. *Colloids and Surfaces B: Biointerfaces* 108:85-89.
- Klemm D, Heublein B, Fink HP, Bohn A (2005). Cellulose: Fascinating biopolymer and sustainable raw material. *Angewandte Chemie International Edition* 44(22):3358-3393.
- Kornblum SS, Stoopak SB (1973). A new tablet disintegrant agent: cross linked polyvinylpyrrolidone. *Journal of Pharmaceutical Science* 62(1):43-49.
- Lanz M (2006). *Pharmaceutical powder Technology: Towards a science based understanding of the behavior of powder system*. Inaugural dissertation pp 13-31
- Lau KK, Jawaid M, Ariffin (2017). Isolation and characterization of microcrystalline cellulose from roselle fibers. *International Journal of Biological Macromolecules* 103:931-940.
- Lee SY, Mohan DJ, Kang In A, Doh GH, Lee S, Han SO (2009). Nanocellulose reinforced PVA composite films: Effects of acid treatment and filler loading. *Fibers and Polymers* 10(1):77-82.
- Liu Y, Liu A, Ibrahim SA, Yang H, Huang W (2018). Isolation and characterization of microcrystalline cellulose from pomelo peel. *International Journal of Biological Macromolecules* 111:717-721.
- Mandal A, Chakrabarty D (2011). Isolation of nanocellulose from waste sugarcane bagasse (SCB) and its characterization. *Carbohydrate Polymers* 86(3):1291-1299.
- Mathew AP, Oksman K, Sain M (2006). The effect of morphology and chemical characteristics of cellulose reinforcements on the crystallinity of polylactic acid. *Journal of Applied Polymer Science*, 101(1):300-310.
- Mohammed BB, Isah AB, Ibrahim MA (2009). Influence of compaction pressures on modified cassava starch as a binder in paracetamol tablet formulation. *Nigerian Journal of Pharmaceutical Science* 8(1):80-88.
- Mood SH, Golfeshan HH, Tabatabaei M, Jouzani GS, Najafi GH, Gholami M, Mehdi Ardjmand M (2013). Lignocellulosic biomass to bioethanol, a comprehensive review with a focus on pretreatment. *Renewable and Sustainable Energy Reviews* 27:77-93.
- Musiliu A, Essien G, Uwah TO, Umoh R, Inibong J, Jackson C (2014). Evaluation of the release properties of microcrystalline cellulose derived from *Saccharum Officinarum* L. in paracetamol Tablet formulation. *Journal of Pharmaceutical Sciences and Research* 6(10):342-346.
- Nishiyama Y (2009). Structure and properties of the cellulose microfibril. *Journal of wood Science* 55(4):241-249.
- Nuruddin M, Chowdhury A, Haque SA, Rahman MM, Farhad SF, Sarwar Jahan M, Quaiyyum A (2011). Extraction and characterization of cellulose microfibrils from agricultural wastes in an integrated biorefinery initiative. *Cellulose Chemistry and Technology* 45(5-6):347-354.
- Nwadiogbu JO, Igwe AA, Okoye NH, Chime CC (2015). Extraction and Characterisation of microcrystalline cellulose from mango kernel: A waste management approach. *Der Pharma Chemica* 7(11):1-7.
- Nwajioji CC, Otaigbe JOE, Oriji O (2018). A comparative study of microcrystalline cellulose isolated from the pod husk and stalk of fluted pumpkin. *Chemical Science International Journal* 25(4):1-11.
- Ofoefule SI (2006). *Textbook of pharmaceutical technology and Industrial Pharmacy*, Sam-Akin Nigeria Enterprises, Lagos, pp.24-68.
- Ogbonna O, Omotoso AE, Nwaneli Christiana N (2016): Production, Characterisation and Evaluation of Tablets obtained from microcrystalline cellulose Obtained from *Pennisetum purpureum*. *Academia Journal of Biotechnology* 4(9):319-324.
- Ohwoavworhwa FO, Adelakun TA (2005). Some physical characteristics microcrystalline cellulose obtained from raw cotton *Cochlospermum planchonii*. *Tropical Journal of Pharmaceutical Research* 4(2):501-507.
- Ohwoavworhwa FO, Adelakun TA (2010). Non-wood fibre production of microcrystalline cellulose from *Sorghum caudatum*: Characterization and tableting properties. *Indian Journal of Pharmaceutical Sciences* 72(3):295-301
- Ohwoavworhwa FO, Ogah E, Kunle OO (2005). Preliminary investigation of physicochemical and functional properties of alpha cellulose obtained from waste paper-A potential pharmaceutical Excipient. *Journal of Raw Materials Research* 2:84-93.
- Ohwoavworhwa FO, Kunle OO, Ofoefule SI (2004): Extraction and characterization of microcrystalline cellulose derived from *Luffa cylindrical* plant. *African Journal of Pharmaceutical Research and Development* (1):1-6.
- Okhamafe AO, Ejike EN, Akinrinola FF, Ubane-Ine D (1995). Aspect of tablet disintegrant properties of cellulose derived from Bagasse and maize cob. *Journal of Pharmaceutical Science* 1:20-29.
- Okhamafe AO, Igboechi A, Obaseki TO (1991). Celluloses extracted from groundnut shell and rice husks 1. Preliminary Physicochemical characterization. *Pharmacy World Journal* 8(4):120-130.
- Okonkwo EU, Ubani ON (2007). Indigenous technologies for the dehulling, storage and utilization of breadfruit seeds *Artocarpus altilis* (Park) Fosb. (*Treculia Africana*Decne) Family: Moraceae in Anambra state. *Journal of Agricultural Research* 4(1):27-30.
- Olorunsola EO, Bhatia PG, Tytler BA, Adikwu MU (2016). Hydration and swelling dynamics of some tropical hydrophilic polymers. *Nigerian Journal of Pharmaceutical Science* 15(1):41-47.
- Oluwasina O, Lajide L, Owolabi B (2014). Microcrystalline cellulose from plant wastes through Sodium hydroxide-Anthraquinone-Ethanol pulping. *Bioresources* 9(4):6166-6192.
- Pachau L, Mali C, Ramdinsangi H, Nirmal KN (2014). Physicochemical and functional characterization of microcrystalline cellulose from bamboo (*Dendrocalamus longispatus*). *International Journal of Pharmtech Research* 5(4):1561-1571.
- Pachau L, Vanlalfakawma DC, Tripathi SK (2014). Muli bamboo (*Melocanna baccifera*) as a new source of microcrystalline cellulose. *Journal of Applied Pharmaceutical Science* 4(11):087-094.
- Raveendran K, Ganesh A, Khilar KC (1995). Influence of mineral matter on biomass pyrolysis characteristics. *Fuel* 74(12):1812-1822.
- Rosa SML, Rehman N, De Miranda MIG, Nachtigall SMB, Bica CID (2012). Chlorine-free extraction of cellulose from rice husk and whisker isolation. *Carbohydrate Polymers* 87(2):1131-1138.
- Rosnah MS, Astimar AB, Wan Hasamudin WH, Gapor AMT (2009). Solid-state characteristics of microcrystalline cellulose from oil palm empty fruit bunch fibre. *Journal of Oil Palm Research* 21:613-620.
- Rubinstein ME (1996). Tablet, In: *Pharmaceutics- the science of dosage form design* (EDME Aulton), Churchill Livingstone 600-615.
- Shanmugam N, Nagarkar RD, Kurhade M (2014). Microcrystalline cellulose powder from banana pseudostem fibres using biochemical route. *Indian Journal of Natural Products and Resources* 6(1):42-50.
- Stamm AF(1964). *Wood and Cellulose Science*. The Ronald Press Company, New York, pp. 132-165.
- Sumaiyah, Basuki W, Karsono (2016). Utilization of microcrystalline cellulose of sugar palm bunches (*Arengapinnata* (Wurmb) maerr.) as Excipients Tablet compression. *International Journal of Pharmtechnology Research* 9(7):130-139.
- Qian Y, Qin Z, Vu NM, Guolin T, Frank Chin YC (2012). Comparison of nanocrystals from tempo oxidation of bamboo, softwood, and cotton linter fibers with ultrasonic-assisted process. *Bioresources* 7(4):4952-4964.
- Nwabueze TU, Otunwa U (2006). Effect of supplementation of African breadfruit (*Treculia africana*) hulls with organic wastes on growth characteristics of *Saccharomyces cerevisiae*, *African Journal of Biotechnology* 5(16):1494-1498.
- Umeh ONC, Nworah AC, Ofoefule SI (2014). Physico-chemical properties of Microcrystalline cellulose derived from Indian Bamboo (*Bambusa vulgaris*). *International Journal of Pharmaceutical Sciences Review and Research* 29(2):5-9.
- Vora RS, Shah YD (2015): Production of microcrystalline cellulose from corn husk and its evaluation as Pharmaceutical Excipient. *International Journal of Research and Scientific Innovation* 2(11):69-74.
- Wu JS, Ho HO, Sheu MT (2011). A statistical design to evaluate the influence of manufacturing factors on the material properties and functionalities of microcrystalline cellulose. *European Journal of Pharmaceutical Science* 12(4):417-425.

- Yusrina RRRK, Sutriyo, Suryadi H (2018). Preparation and characterization of microcrystalline cellulose produced from Betung Bambo (*Dendrocalamus asper*) through Acid Hydrolysis. *Journal of Young Pharmacists* 10 (2): S79-S83
- Zhbankov RG (1962). Infra red spectra of cellulose and its derivatives. *Science and Technic*, p 333.